International Journal of Civil Engineering (IJCE)
ISSN(P): 2278-9987; ISSN(E): 2278-9995
Vol. 5, Issue 1, Dec - Jan 2016, 69-82

International Academy of Science, Engineering and Technology
Connecting Researchers; Nurturing Innovations

ENHANCED METHOD OF PARTICLE IMAGE VELOCIMETRY APPLIED TO MEASURE THE SCOUR PHENOMENA IN BRIDGE PIERS

ANTONIO CAMPA-RODRIGUEZ[1], FERNANDO RAFAEL ASTORGA-BUSTILLOS[2], CORNELIO ALVAREZ-HERRERA[3], JOSE G. MURILLO-RAMIREZ[4] & GUADALUPE ESTRADA-GUTIERREZ[5]

[1,2,3,5]Universidad Autónoma de Chihuahua, Facultad de Ingeniería, Nuevo Campus Universitario, Circuito Universitario S/N, C.P, Chihuahua, Chih., México

[4]Centro de Investigación en Materiales Avanzados S. C., Miguel de Cervantes 120, Complejo Industrial Chihuahua. C.P, Mexico

ABSTRACT

In this work is reported an enhanced methodology of the particle image velocimetry (PIV) developed to measure the velocity of soil particles in real time with the purpose to study and analyze in high detail the phenomenon of scour in piers of bridges. It was used a lab model representing a pier of bridge by using a cylindrical bar inside of a rectangular water channel with transparent walls, provided with an electric pump to create a controlled water flux. A layer of selected white sand was deposited on the bottom of the water channel in order to simulate a flow of a mixture of water and soil impacting over the cylindrical bar representing the pier of bridge. The movements of particle in the flux of fluid lit by a sheet of light layer was recording in video format using a high resolution camera with an acquisition velocity of 164 images per second and caption of 404 x 244 pixels. From the videos acquired were obtained the velocity vectors of soil particles in the water flow which originate the scour effect in the bridge pier using specialized software. These velocity vectors of soil particles were used to represent graphically in real time the scour velocity distribution that occurs at the moment of erosion of soil at the bottom of pier. One of the remarkable results of this research shows the presence of an oscillatory movement of water flux around the cylindrical bar, representing the pier of bridge, which originates fatigue to the soil particles in direct contact with the water flux leading in this way to erosion.

KEYWORDS: Bridge Piers, Erosion, Scour, Particles Image Velocimetry

INTRODUCTION

Scour is a natural phenomenon caused by the erosive action of water flowing in rivers and channels. The local scour is the removal of deposits around the structural elements that are found in water flow (Dargahi, 1990). This represents a decrease in the riverbed level due to water erosion, so that there is a trend to expose the foundation of bridges as a result of the erosive action of water courses. As erosion progresses, it undermines the foundations of the structure causing its collapse (Barbhuiya and Dey, 2004; Khwairakpam and Mazumdar, 2006). Bridge collapsing due to the piers or abutments scour is the most common fault. A study of the Federal Road Administration of the United States of North America concluded that in a total of 383 faults in bridges, approximately 25% correspond to damages in their peers and 72% to damages in their abutments (Smith, 1979; Richardson *et al*., 1993 Landers and Mueller, 1996). In case of Mexico there is a lack of studies about the effect of scour in national infrastructure. However, the experience in addressed cases in

different offices related with the infrastructure on land routes enables us to estimate that scouris the cause of about 90% of collapses in bridges (Solares, 1989).

The local scour in piers of bridges is caused by the change on direction in stream lines, turbulence, flow acceleration and the resultant vortexes induced by the water flow obstruction (Raudkivi, 1986). In piers, into the water course, a series of turbulences are produced which make the level of the river to descend specially near these structures. Around piers, a deep pit is formed due to the scour produced by a system of vortexes generated by the interference that the pile causes to the flow as shown in Figure 1. The mechanism that scours produces is associated to the tridimensional separation of flow upstream of the pile and to a periodical vortex at the bottom of it (Dargahi, 1990; Ettema *et al.*, 2010 and Ettema *et al.*, 2011).

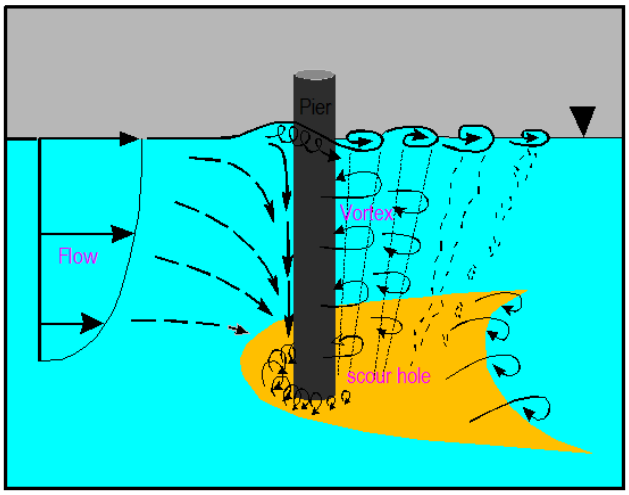

Figure 1: Behavior of Water Flow Interacting Whit a Cylindrical Pier (Ettema et al., 2011)

The analysis of the fields of a flow speed in movement is very important for a variety of aspects in the hydrodynamics and dynamics of fluids. For the basis of experimentation, measures of flow velocity can be essential to the plenty understanding of fluid physics processes. One of the most used methods to measure the speed fields is the one known as particle image velocimetry (PIV) which is a real time, effective and non-intrusive method. (Martinez and Gonzalez, 2003)

PIV is an optical method of flow visualization used in several research areas. Usually this technique is used to measure the instantaneous velocity distribution in a flow plane through the photographic determination of movement of particles in a plane during a very short time period (Cengel and Cimbala, 2006).

The principle of PIV is to measure the distance, Δs, introducing particles in a fluid in movement during a time periodΔt. The U speeds calculated under the following equation:

$$U = \frac{\Delta s}{\Delta t} \quad (1)$$

It is considered that suspended particles in water have the same speed of the flow that transports them. The particles are lit by a source of light (laser) and a camera is used to capture images of the fluid with the lit particles. Δtis equal to the time between each light pulse. The camera is used to record the position of the particles during each light pulse and at least two pulses must be registered.Δ Sis the distance between the two recordings (Cengel and Cimbala, 2006)

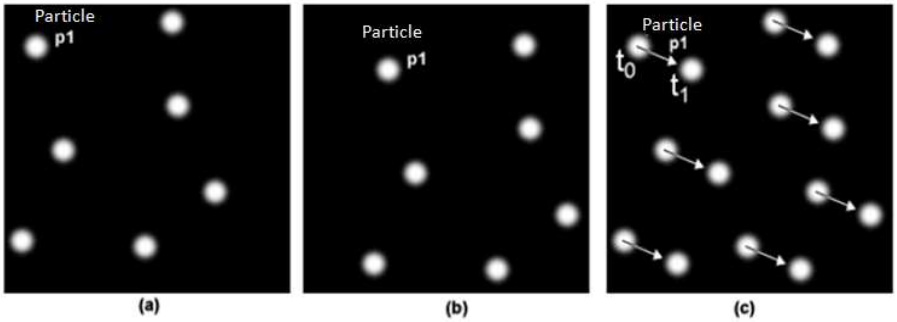

Figure 2: Schema of Images Movement Used in PIV (Adrian, 1991 and Lopez, 2006)

In the images process, the crossed correlation is used to find the most similar position between two images such as is shown in Figures 2(a) and 2(b), corresponding to consecutive images. Next, these kinds of images are processed to determine the individual movement described by the particles between one image and the other. Figure 2 (c) shows movement of each one of these particles which can be seen as a couple of particles going from time $t_0$to time t_1 (Adrian, 1991).

For the evaluation with crossed correlation, PIV images are divided into a little rectangle areas called "interrogation zones". An interrogation zone is a region of an image *f*, that is to say a sub-image of *f*. It is assumed that all the particles that are into an interrogation zone, move in a uniformly movement. The standard algorithm of PIV consists in processing two interrogation zones of the same size and with the same coordinates inside the image. One zone is from the first image and the other from the second image as shown in Figure 3 (Adrian, 1991).The interrogation zones must be processed in order to find an average of movement of particles in the two images. In this way the methodology consists in calculating directly the crossed correlation between the two zones:

$$f(x,y)\odot g(x,y) = \sum_{i=-M}^{M}\sum_{j=N}^{N} f(i,j)g(i+x,j+y) \quad (2)$$

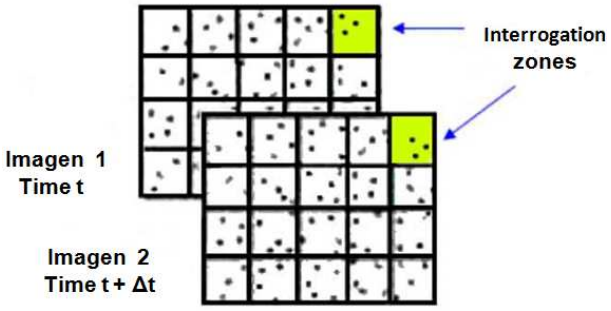

Figure 3: PIV Images Divided in Interrogation Zones (Adrian, 1991andLópez, 2006)

For$x = 0, \pm 1, \pm 2 \ldots\ldots N-1;\ y = 0, \pm 1, \pm 2 \ldots\ldots M-1$,where*f(x, y)* is the sub-image correspondent to the first interrogation zone, *g(x ,y)* is the sub-image associate to the second zone, and M and N are the width and the height in pixels of the interrogation zone, respectively. The process consists in moving a sub-image over the other and adds the products of the values where overlapping occurs. Each value is saved as a matrix called "matrix or plane of crossed correlation", in the position that represents the moving of the second sub-image over the first one.

The goal of this work was to apply an enhanced PIV method to measure the velocity and direction of particles in soil that are scoured in a pile of bridge by using a lab model. The results of this research enable us to establish and

adequate strung methodology to measure the magnitude and direction of instantaneous velocity of soil particles, instead of use the average velocity of soil particles as usually has been considered in the study of scour phenomena in previous models reported in the literature.

MATERIALS AND EQUIPMENT USED

It was used a rectangular channel with a variable pitch of 4.7 m long, 0.15m deep and 0.08 m width, with an electric pump of half horse power. The walls of the channel, as shown in Figure 5, are of transparent acrylic, in order to let the laser light go through, which are mounted over a steel structure and a deposit for providing water with a capacity of 385 liters. A metallic base of 6 cm x 15 cm with a screwed steel bar of 12.7 mm diameter and 9 cm long was used to simulate the effect of a bridge. The camera was calibrated using a square mesh with 0.5 cm per side as shown in Figure 4.

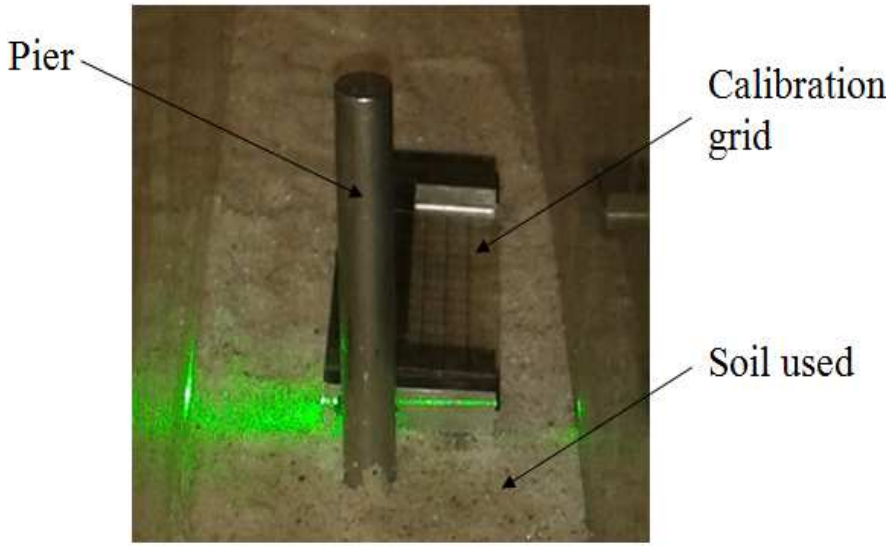

Figure 4: Metallic Bar 12.7 mm Diameter and Calibration Mesh

The water velocity was controlled by varying the longitudinal slop of the channel due to it did not have any gadget to this purpose. Nevertheless, a dissipation screen at the initial edge of the channel to reduce turbulences was installed, whereas in the other edge, was put a steel stopper to generate a uniform tight in the entire length of channel as shown in Figure 5.

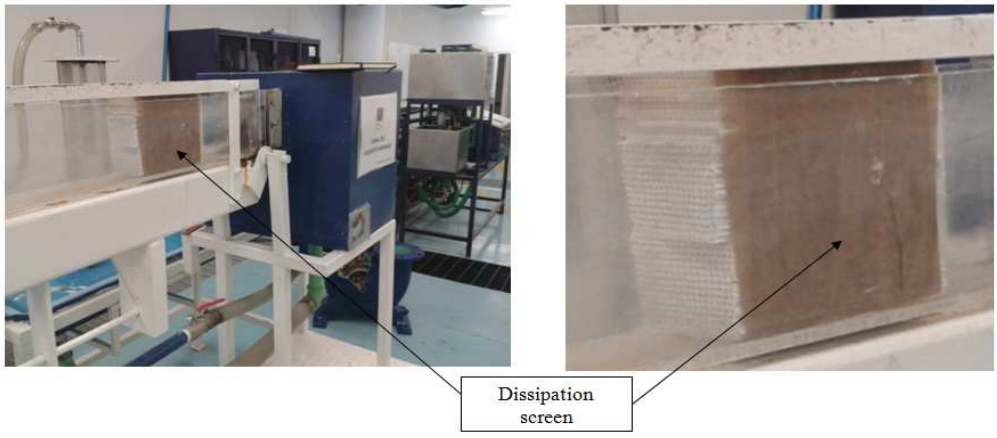

Figure 5: Dissipation Screen to Reduce Turbulences

In order to choice the soil used in the bottom of the channel, several preliminary tests were performed. From this selection was concluded that the material with better performance was a white marble, because it reflected better the laser light regarding to the other samples tested. Figure 6 shows the granulometric curve of the marble used in this research. The marble used had the following granulometric properties: D_{10} = 0.35 mm, D_{30} = 0.6 mm, D_{50} = 0.70 mm, D_{60} = 0.8 mm, C_u = 2.28 and C_c = 1.28. According to the SUCS classification, this material is well graded sand (SW). In fact, particles whit sizes under 0.075mm were eliminated with the purpose to homogenize the grain size of sand used in this study.

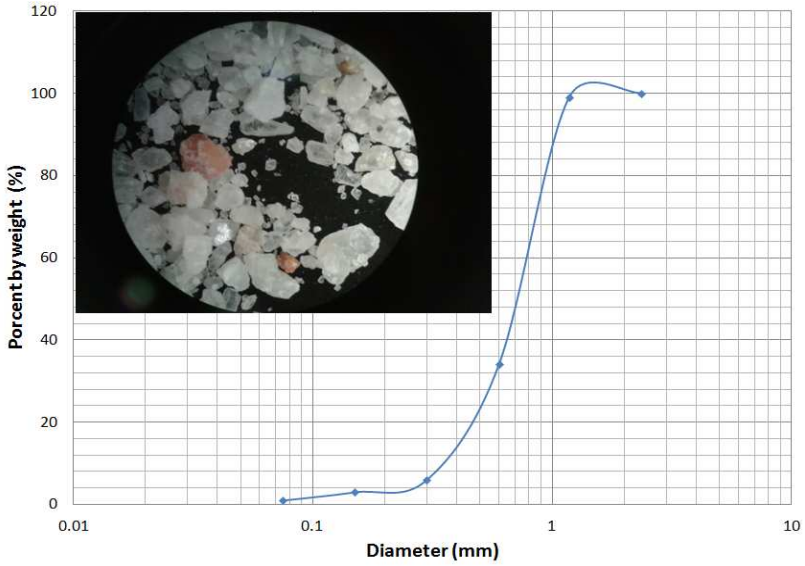

Figure 6: Granulometric Curve of Marble used in this Research

To generate the system of lighting, which is a fundamental part of the PIV system, it was mounted an experimental setup over a steel plate including a laser with an emission at 530 nm, a negative lens of 2.5 cm diameter and a focal length of -25 mm and a cylindrical positive lens with a focal length of 150mm. The lighting system was set in horizontal position over a metallic table of 1.2 m x 1.2 m.

The recording of movement particles in the flux of fluid was performed using a high resolution digital camera (CMOS sensor) with a speed of 164 images per second (38.3 megabits per second) and a caption size of 404 x 244 pixels. The camera was mounted vertically over a metallic plate, fastened by a lens holder mount specially designed to put the camera over the channel, in order to capture the movement of particles in the horizontal plane as shown in Figure 7.

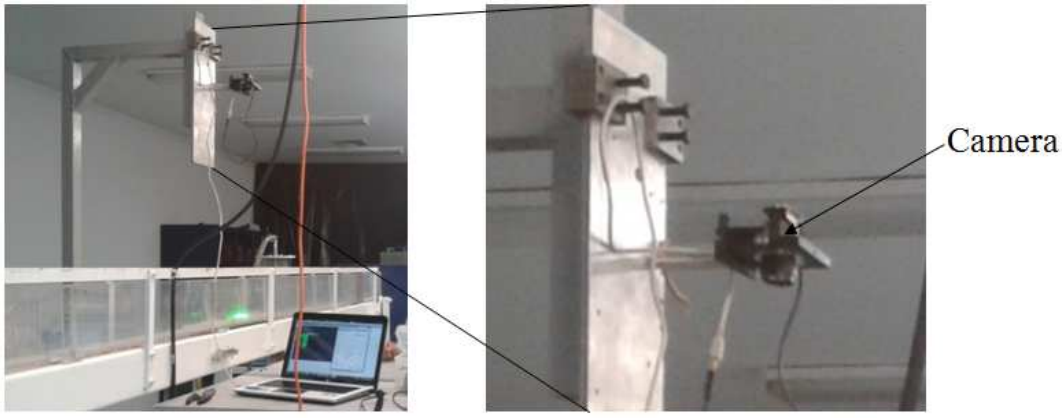

Figure 7: System Used for the Caption and Storage of Images

The final processing of the videos of the particles movement was performed using several software packages including MATLAB version 2012b, Tec Plot 360 version 2006 and "pro VISION PIV" (IDT software)(Martinez Gonzalez A. *et al*,2012).

METHODOLOGY

The experiment was carried out in a darkened area with the purpose of recording the dynamics of particles and water flow by means of the PIV optical setup. A longitudinal slope of zero percent was applied to the water flow in the channel. The experiment was done with an expense of 0.4125 $ls^{-1}$with potable water without any special treatment, an average speed of 0.04261 ms^{-1}, and a level of water equal to 12 cm. The water flow was subcritical with a number of Froude equal to 0.0397.

Over the steel plate a bar was fastened, a layer of soil of 2.5 cm thickness was put uniformly along the total length of the steel plate equal to 150 m upstream and downstream of the metallic bar as shown in Figure 8. The laser lighting system was installed over a metallic table put in from of the channel, exactly at the same high of its base. Figure 9 shows a diagram of the lighting system used in this research.

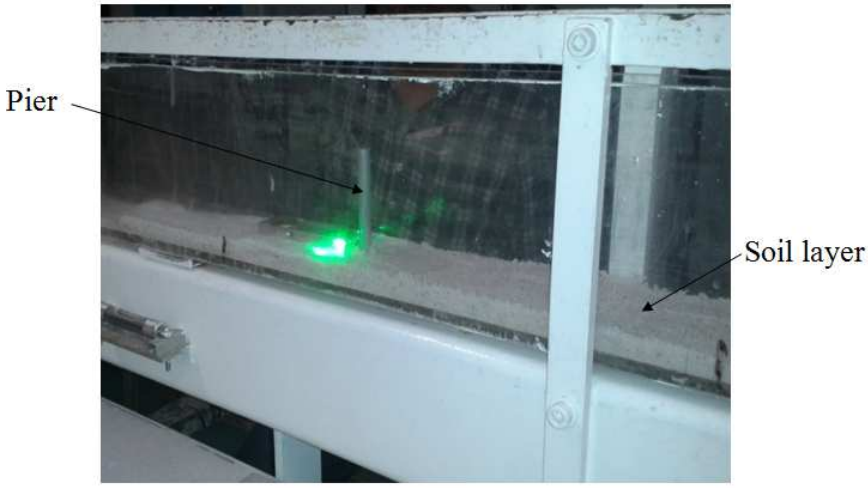

Figure 8: View of the Pier Model

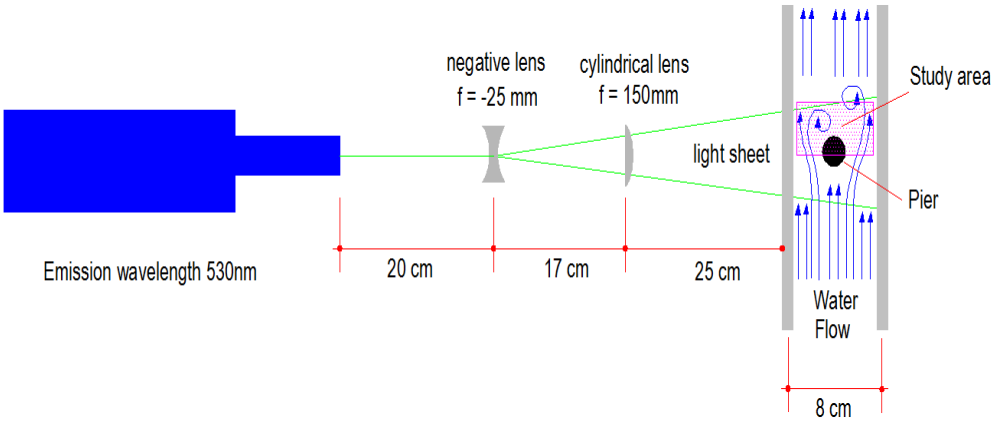

Figure 9: Top View of the Scheme of Lighting Setup and the Plant Channel

The cylindrical and negative lenses opened the laser light beam to form a layer of light in a horizontal plane. This light was projected in front of the base of the metallic bar, so that the soil particles that surrounded it were perfectly illuminated. In this way, was possible to study the behavior of the water flow, during the interaction between soil and the metallic bar that simulates a pier. The camera was mounted in a metallic structure at 75 cm above the channel to capture the images in the same horizontal plane of the light layer. Before capturing the images, a calibration process using a grid of 0.5 cm per side was done. The calibration used was of one pixel, equivalent to 0.095 mm as shown in Figure 4.

The images of the water flux dynamics occurring in the horizontal plane of light layer were captured by using the camera mounted in perpendicular direction of water flux, in a metallic structure at 750 mm above over the level of water in the channel. The light layer was projected in the frontal part of the cylindrical metallic bar at different heights from the bottom of the water flow, equals to 5 mm, 10 mm, 15 mm, and 20 mm. For each case in particular, were taken several images in order to obtain the correct information about the dynamics of water flow. Figure 10shows a detailed schema of the levels where the layer of light was projected.

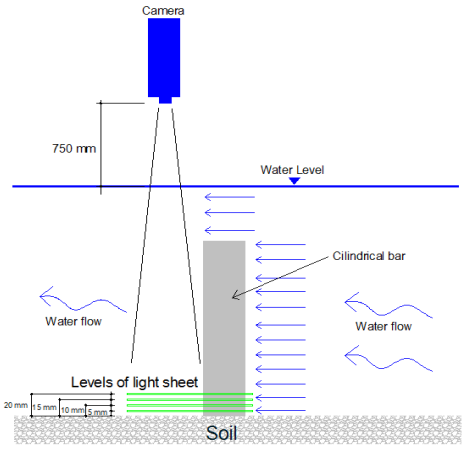

Figure 10: Levels where the Laser Layer of Light was projected

For each one level of the light layer, different videos were obtained and then processed using a program writing to run in MATLAB version 2012b.The videos were fragmented into images which were later processed by another program writing in MATLAB to convert them in images type BMP. The statistic technique used for the processing of images was the crossed correlation by using the software pro VISION PIV. From this analysis were obtained the numeric values of the velocity of the material moved by the water flow at different heights over the bottom of the channel. As the last step in the processing of the results it was made a graphic representation of the velocity vectors both in the axial (Ux) and the transverse plane (Vy) of the soil particles using the program Tec plot 360 version 2006.

RESULTS AND DISCUSSIONS

A series of consecutive images of the displacement of soil particles at an acquisition rate of 164 images per second were obtained after to analyze the four videos corresponding to the four heights (5,10,15 and 20 mm) considered regarding to the bottom of the channel at which the laser light layer was projected. The velocity vectors of soil particles were obtained from the analysis of an area of 130 by 140 pixels. Figure 11 show graphically the method used to detect the movement of particles via the superposition of pairs of particles images processed by using the specialized software used in this study. The particles were represented in white color before their displacement and in black color after their displacement in order to represent their resultant movement in blue color as shown in Figure 11.From the fragmented

images of the videos obtained at each depth of light layer level considered, the velocity vectors of soil particles scoured by the effect of pile and the water flow were obtained. In this way, using the velocity vectors of particles was possible to represent graphically in real time the scour velocity distribution that occurs at the moment of erosion of soil at the bottom of pile.

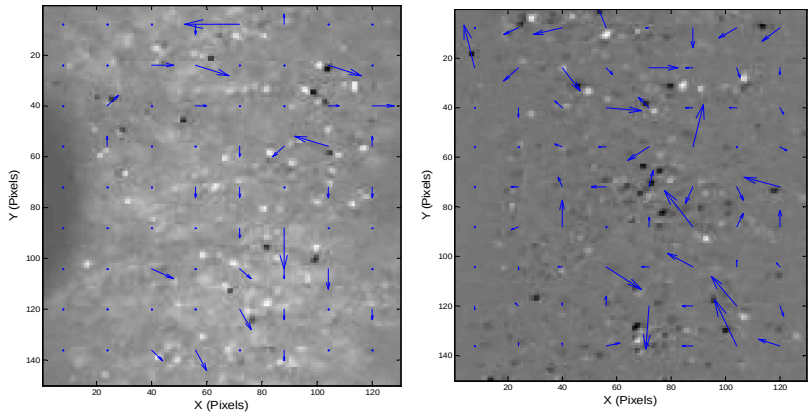

(a) **(b)**

Figure 11: Caption of Velocity Vectors of soil Particles Surrounding the Pier at (a) 5 mm, and (b) 20 mm Height Regarding to the Bottom of Channel, Respectively

Some of the more important results of this research that represent the magnitude of the velocity vectors in both, axial (along the length of channel) and transverse (perpendicular to the direction of water flow) direction, corresponding to different heights regarding to the bottom of the channel at which the laser light layer was projected are shown in Figures 12 to 15. These figures correspond to a specific value of time included in the total data acquisition interval of time. In Figures12 to 15, the 2D contours show the magnitude distribution of both average velocities, axial U and transverse V, and in addition its direction represented by the arrows included in the images. On the other hand, the 3D images of Figures 12 to 15 represent the spatial distribution of both velocities axial U and transverse V, showing its magnitude in the z direction.

As shown in the 3D images included in Figures 12 to 15 the pile produces a non uniform separation of water flow. It is interesting to observe from these 3D images how in front of pile are generated vectors of negative velocity (regarding to the origin placed at the front of the cylindrical bar representing the bridge pier) that generate a sort of vortex which originates the erosion of the pier of bridge by the soil particles. In fact, it can be observed in Figures 12 to 15that the axial velocities distribution has low amplitude at the right side of channel, which is due to a higher storage of material in the left side regarding to the right side of channel during the erosion process.

From the images shown in Figures 12 to 15 it can be observed that the negative direction of the velocity vectors generates an oscillatory movement of the water flux which in turn originates fatigue to the soil particles in direct contact with the water flux, inducing the effect of erosion over the pier. It is also interesting to note from the typical results shown in Figures 12 to 15 how the magnitude of both average velocities, axial and transverse, varies with a nonlinear behavior depending on the height regarding to the bottom of the channel. In fact, it was found a parabolic increase of the maximum magnitude of both average velocities, axial and transverse, when the height of light sheet regarding to the bottom of the channel is also increased as shown in Fig. 16.

Usually the existent methods developed to describe the scour phenomenon consider the average velocity of water

flux of the section under study. However, in this work the enhanced PIV method employed to describe the scour phenomenon in a pile of bridge is able to measure the velocity of soil particles as a function of time. This open the possibility to study the scour phenomena in high detail due to it is possible to analyze completely, in real time, the flow dynamics of water and soil particles present in the experimentation channel. A representative result obtained in this direction during a typical interval of acquisition data time is shown below. Figure 17(a) and (b)show the temporal behavior of both maximum average velocities, axial and transverse, at heights of light sheet equal to 5 mm and 10 mm, regarding to the bottom of the water flow considered in this work, respectively, corresponding to a fixed point with coordinates x = - 2.05 pixel, and y = 0.65 pixel. Figure 17 (c) and (d) show the temporal behavior of both maximum average velocities, axial and transverse, at heights of light sheet equal to 15 mm and 20 mm corresponding to a fixed point with coordinates x = -443.4 pixel, and y = 386.0 pixel. As can be seen in Figure 17 the magnitude of axial and transverse average velocities strongly varies in time. Nevertheless, this variation on the magnitude of both velocities is strongest for the higher heights of light sheet regarding to the bottom of the channel.

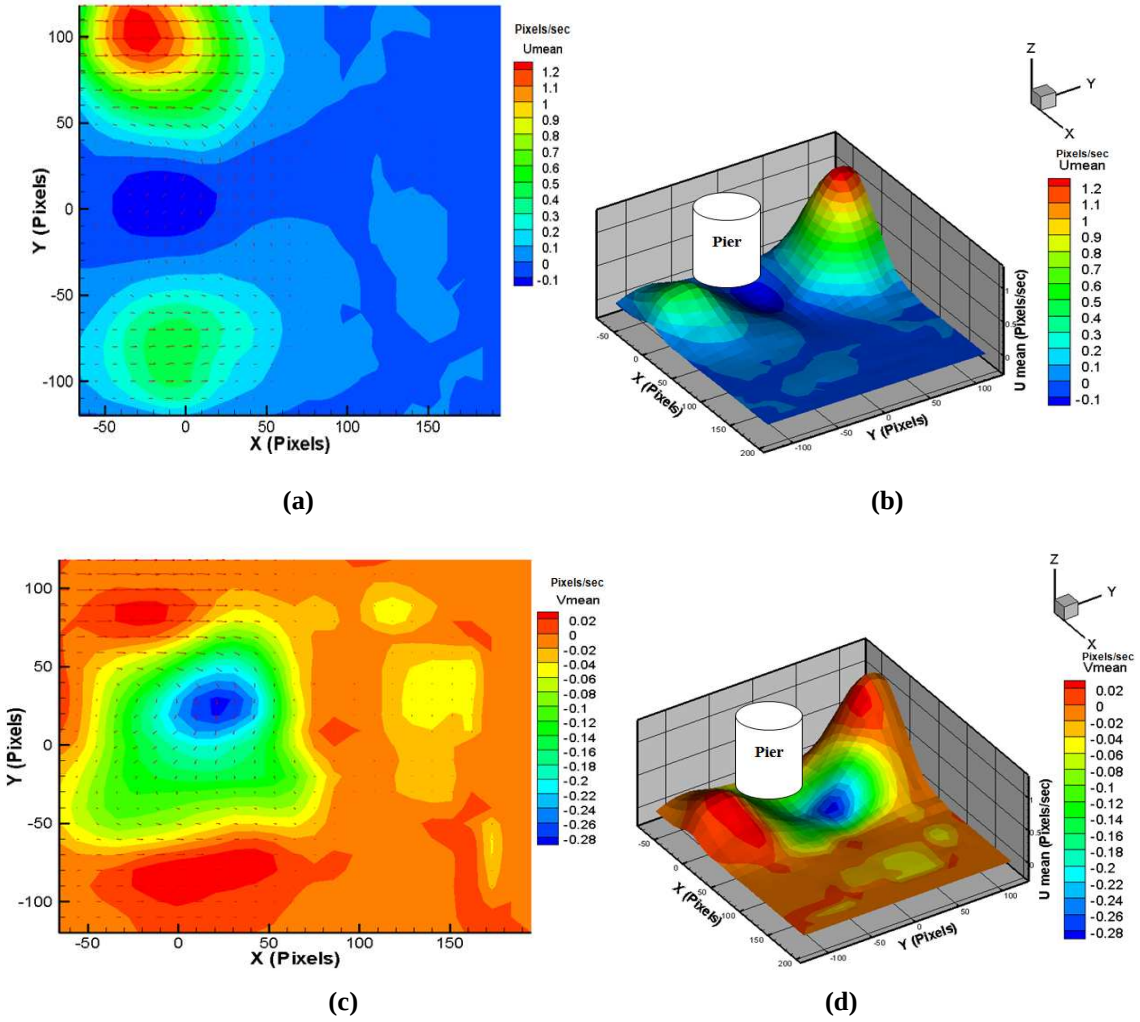

Figure 12: (a) 2D Contour Distribution of the Axial Velocity Vectors$\vec{U}x$ at 5 mm Height, (b) 3D Representation of the Average Magnitude of Axial Velocity Vectors, (c) 2D Contour Distribution of the Magnitude of $\overrightarrow{Vy}$ Transverse VelocityVectors at 5 mm Height and (d) 3D Representation of the Average Transverse Magnitude of Velocity Vectors

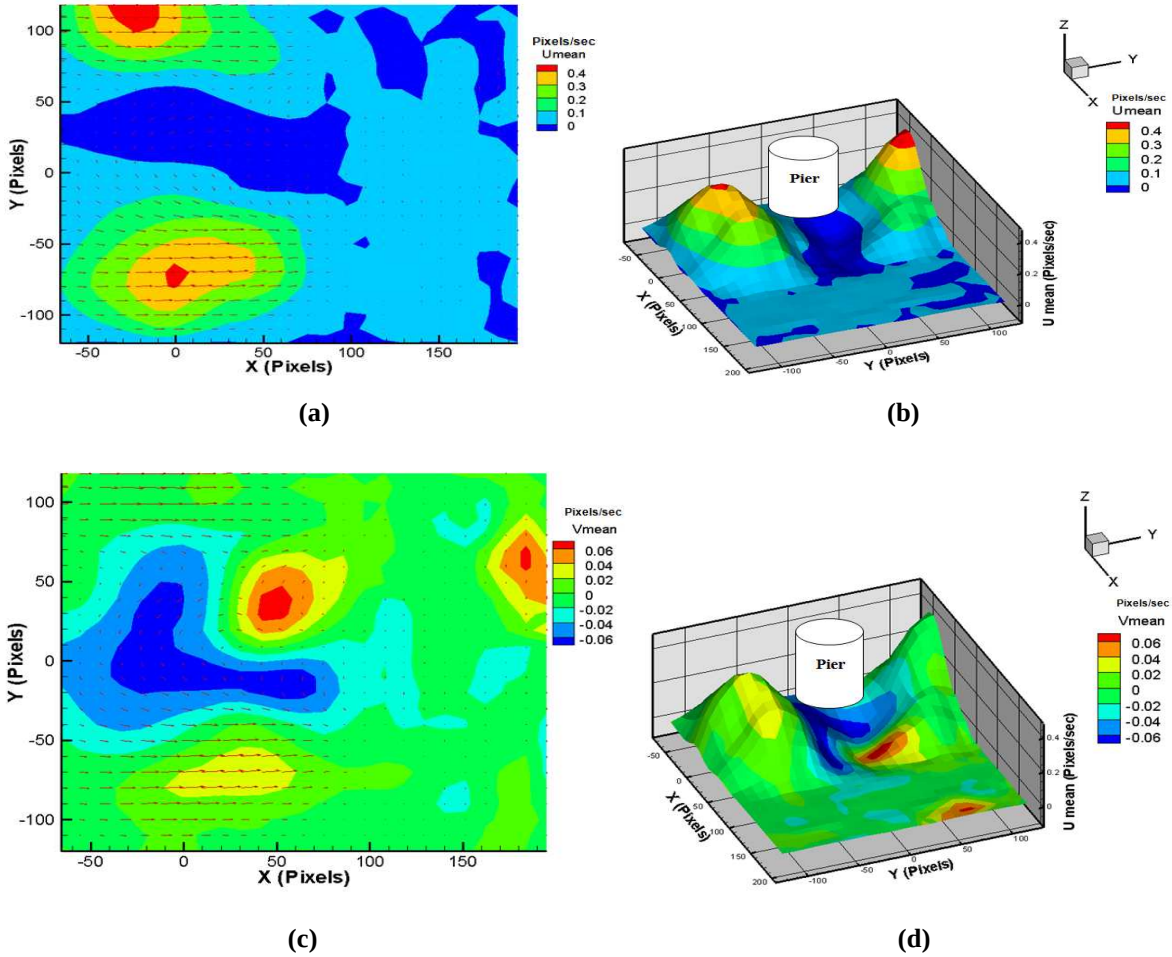

Figure 13: (a) 2D Contour Distribution of the Magnitude of $\overrightarrow{Ux}$ Axial Velocity Vectors at 10 mm Height, (b) 3D Representation of the Average Magnitude of Axial Velocity Vectors, (c) 2D Contour Distribution of the Magnitude of $\overrightarrow{Vy}$ Transverse Velocity Vectors at 10 mm Height End (d) 3D Representation of the Average Transverse Magnitude of Velocity Vectors

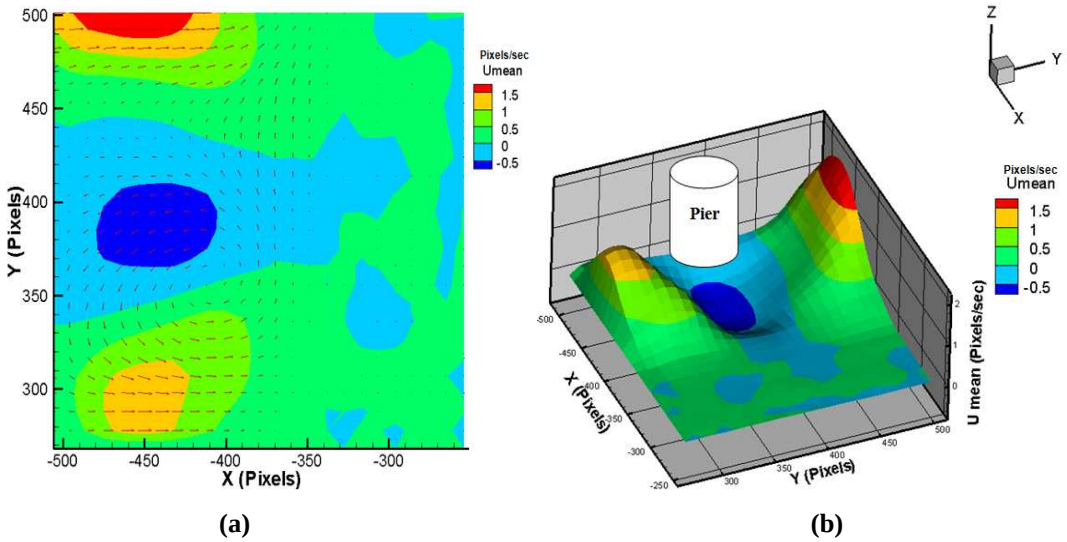

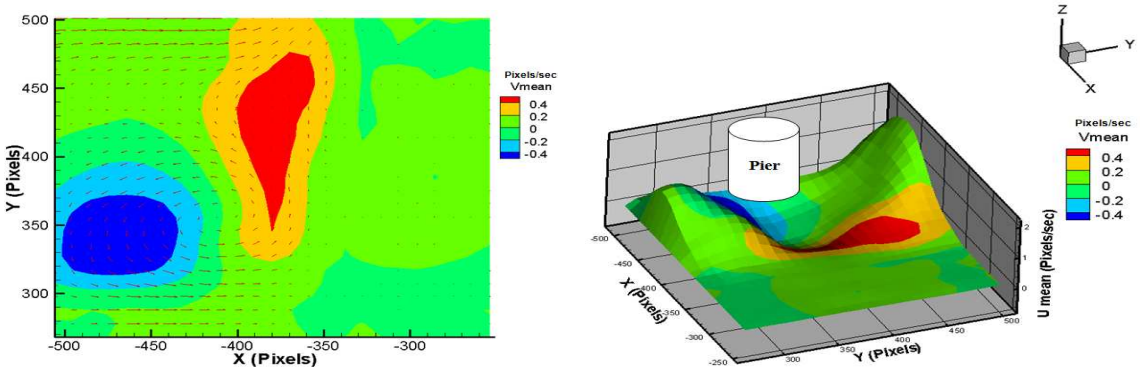

(c) **(d)**

Figure 14: (a) 2D Contour Distribution of the Magnitude of $\vec{U}x$ Axial Velocity Vectors at 15 mm Height, (b) 3D Representation of the Average Magnitude of Axial Velocity Vectors, (c) 2D Contour Distribution of the Magnitude of $\overrightarrow{Vy}$ Transverse Velocity Vectors at 15 mm Height and (d) 3D Representation of the Average Transverse Magnitude of Velocity Vectors

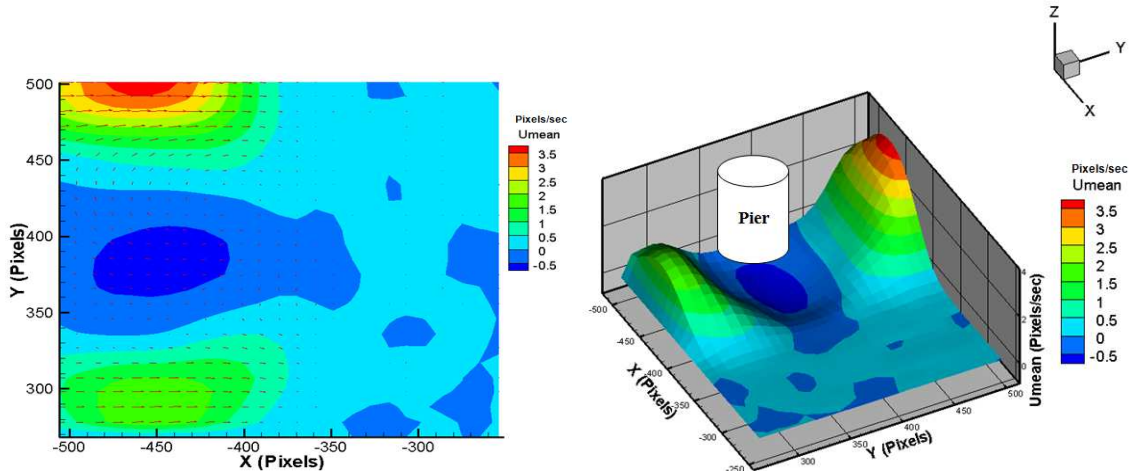

(a) **(b)**

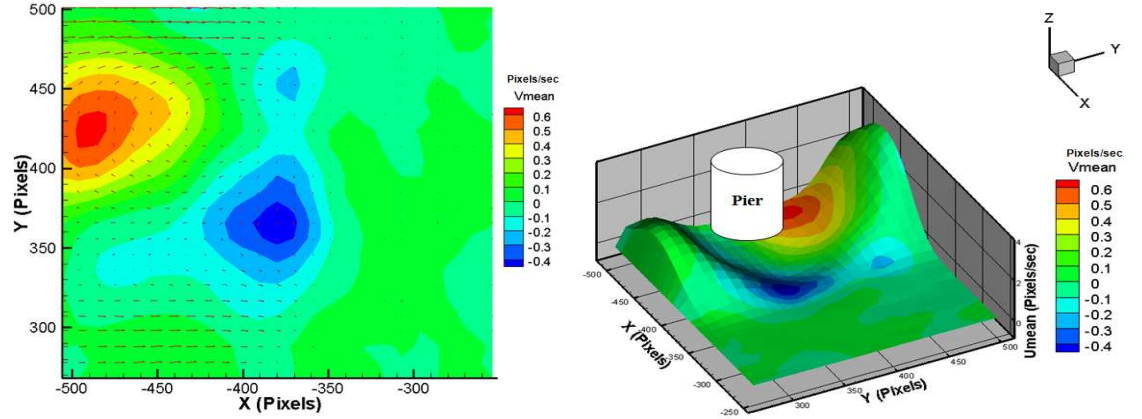

(c) **(d)**

Figure 15: (a) 2D Contour DISTRIBUTION of the magnitude of $\vec{U}y$ Axial Velocity Vectors at 20 mm Height, (b) 3D Representation of the Average Magnitude of Axial Velocity Vectors, (c) 2D Contour Distribution of the Magnitude of $\overrightarrow{Vx}$ transverse velocity vectors at 20 mm Height and (d) 3D Representation of the Average Transverse Magnitude of Velocity Vectors

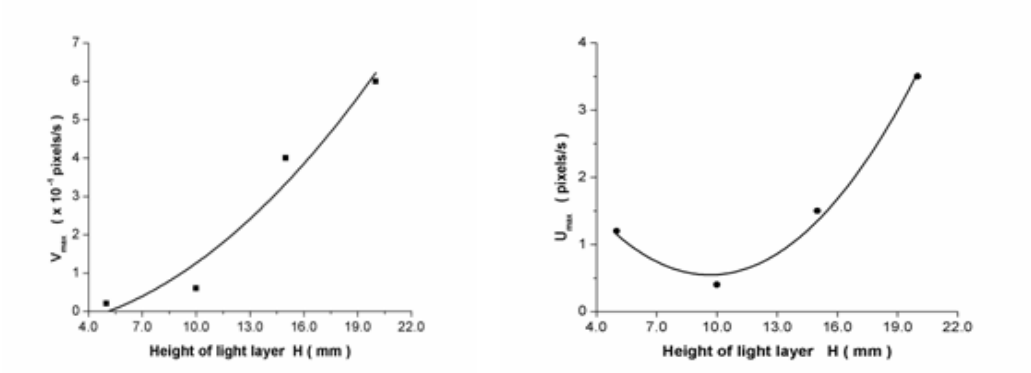

(a) **(b)**

Figure 16: (a) Maximum axial speed (Umax), and (b) maximum transverse speed (Vmax), as a Function of the Height of Light Sheet The continuous Line Represent the Better Fitted Parabolic Curve, Umax = 3.15 -0.54*H +0.028*H^2, and Vmax = -0.05 + 0.0016*H + 0.016*H^2, Respectively

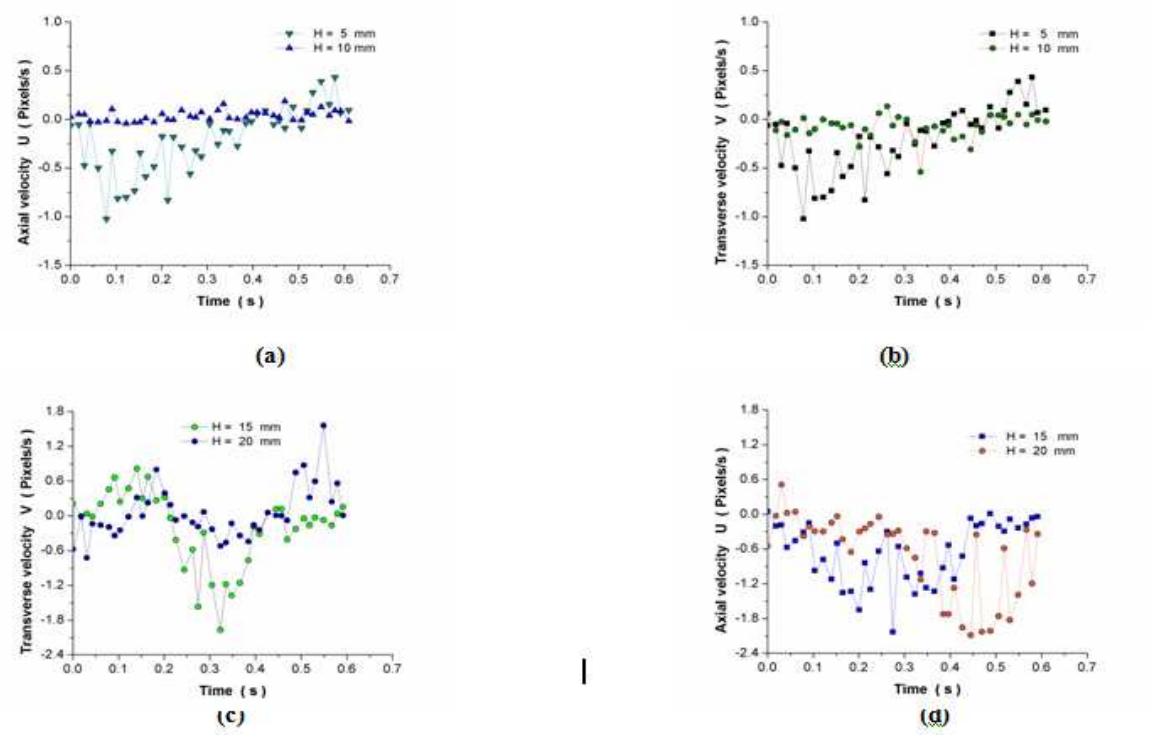

(a) **(b)**

(c) **(d)**

Figure 17: Temporal Behavior of Maximum Average Axial (a) and (c), and Transverse (b) and (d) Velocities. The height of Light Sheet is Equal to 5 mm and 10 mm regarding to the Bottom of the Water Flow Considered for (a) and (b), and 15mm and 20mm for (c) and (d) Figures (a) and (b) Correspond to a Fixed Point with Coordinates x = - 2.05 pixel, y = 0.65 pixel; (c) and (d) Correspond to a Fixed Point with Coordinates x = -443.4 Pixel, and y = 386.0 Pixel

CONCLUSIONS

In conclusion, by means of the methodology developed in this research it was possible to measure the speed of soil particles in real time, which give the possibility to study and analyze the phenomenon of scour with high detail. An oscillatory movement of the water flux was deduced from the change on the direction of the velocity vectors found from

the results obtained in this study. This oscillatory movement in turn originated fatigue to the soil particles in direct contact with the water flux, inducing in this way an erosion effect around the pier. It is also found that the magnitude of both average velocities, axial and transverse, varied with a nonlinear behavior depending on the height regarding to the bottom of the channel. In fact, it was found a parabolic increase of the maximum magnitude of both average velocities, axial and transverse, when the height of light sheet regarding to the bottom of the channel is also increased.

It is expected that the obtained results in this research can lead to propose new techniques which allow understanding the erosion effects induced by the flow of water and soil particles over the bridge piles. This is of high relevance due to currently the failures by scour in bridges are still the main cause of the collapse of these structures.

ACKNOWLEDGEMENTS

The authors want to thank to Faulted de Ingeniería de la Universidad Autónoma de Chihuahua, CONACyT for the support to perform this research under Doctoral Program in Engineering, and Centro de Investigacionesen Optica A. C. (CIO) of León Guanajuato city for assistance in image processing

REFERENCES

1. Adrian R. J. (1991). Particle-imaging techniques for experimental fluid mechanics. Annu. Rev. Fluid Mech. 23: 261-304
2. Barbhuiya A. K. and Dey S., (2004). Local scour at abutments: A review. Department of Applied Mechanics, National Institute of Technology and Department of Civil Engineering, Institute of Technology, Indian.
3. Cengel and Cimbala, (2006). Fluid Mechanics: fundamentals and applications. McGraw-Hill series in mechanical engineering.
4. Dargahi B. (1990). Controlling Mechanism of Local Scour. Journal of Hydraulic Engineering. ASCE. Vol. 116. N° 10. pp 1197-1213.
5. Ettema R., Nakato, T. and Muste, M., (2010). Estimation of Scour Depth at Bridge Abutments. Final Report, NCHRP 24-20, Transportation Research Board, Washington, DC.
6. Ettema R., Constantinescu G. and Melville B. (2011). Report for NCHRP Project 24-27(01) National Cooperative Highway Research Program.
7. Khwairakpam P. and Mazumdar A. (2006). Local Scour Around Hydraulic Structures, International Journal of Recent Trends in Engineering, Vol. 1, No. 6.
8. Landers M.N. and D.S. Mueller. (1996). Channel Scour at Bridges in the United States Federal High Way Administration, Report Number FHWA/RD-95/18.
9. López H. M., (2006). “Un Nuevo algoritmo en la técnica de velocimetría por imágenes de partículas. Máster in Science Disertación, Instituto Politécnico Nacional. Centro de investigación en computación.
10. Martínez J.D. y González F.J. (2003). Velocimetría de partículas basado en imágenes digitales. Instituto de Investigación en Comunicación, San Luis Potosí, SLP, México.

11. Martínez-González A., Guerrero-Viramontes J. A., and Moreno-Hernández D. (2012). Temperature and velocity measurement fields of fluids using a schlieren system. Appl. Optics, Vol. 51, No. 16, pp. 3519-352.
12. Raudkivi A. J. (1986). Functional Trends of Scour at Bridge Piers. Journal of Hydraulic Engineering. ASCE. Vol. 112. N° 1, pp 1-13.
13. Richardson E. V., Harrison L. J., Richardson J. R., Davies S. R. (1993). Evaluating scour at bridges. Publ. FHWA-IP-90-017, Federal Highway Administration, US Department of Transportation, Washington, DC.
14. Smith D.W. (1979). Institution of civil engineers Proceedings, Part. 1, Vol. 6 pp. 367-382.
15. Solares D.C. (1989). La Socavación en Puentes y Obras Menores. Reunión Conjunta sobre Socavación en Puentes y Obras Menores de la AMH, AMIVITAC y SMMS. México.